23rd ABCM International Congress of Mechanical Engineering
December 6-11, 2015, Rio de Janeiro, RJ, Brazil

COMPUTATIONAL SIMULATION OF THE FLOW-INDUCED VIBRATION OF A HYDRAULIC TURBINE STAY VANE

Renato Venturatto Junior
Bruno Souza Carmo
Escola Politécnica da USP – Av. Prof Luciano Gualberto, Travessa 3 nº 380, Butantã, São Paulo,05508-010, Brasil
renatovj@usp.br
bruno.carmo@usp.br

Abstract. *This article presents a methodology developed to perform a detailed computational simulation of the flow-induced vibration of a hydraulic turbine stay vane. The flow around the vanes was computed using a commercial CFD code, ANSYS Fluent, and the calculation of the structural response and its coupling with the flow equations was done with User Defined Functions. With this methodology, the structural response of the vane for a range of operational flow conditions can be analyzed, and the situations for which resonance occurs can be identified. A proper design of the vane should avoid such situations, because they can lead to structural failure or decrease of the vane's service life. The methodology developed has the advantage of helping the design of such components without depending excessively on experimental methods or empirical rules. Also, it allows either modifying existing profiles or choosing the best shape for new ones based on the best manufacturing criteria.*

Keywords: *Hydraulic Turbines, Fluid-Structure Interaction, Flow-Induced Vibration, Computational Simulation.*

1. INTRODUCTION

The problem of vortex-induced vibration in different components of hydraulic turbines has been studied and discussed by many authors. Regarding the stay vane (see Figure 1), one can mention mainly Gissoni (2005) and Kurihara et al. (2007), whose works have as main approach to modify the trailing edge either machining a chamfer or performing another modification that narrows this edge. Some recent works, as Yao, *et al* (2014) and Zobeiri, et al. (2009), try to show as well the influence of the trailing edge on the vibration of the structure. Both use a NACA 0009 profile to compare empirically a Donaldson trailing edge (oblique) to a blunt trailing edge and the results once more prove that narrow trailing edges undergo smaller vibrations. Most part of the actions taken into account in order to avoid such vibrations are, as showed above, either empirical or based on previous experiences.

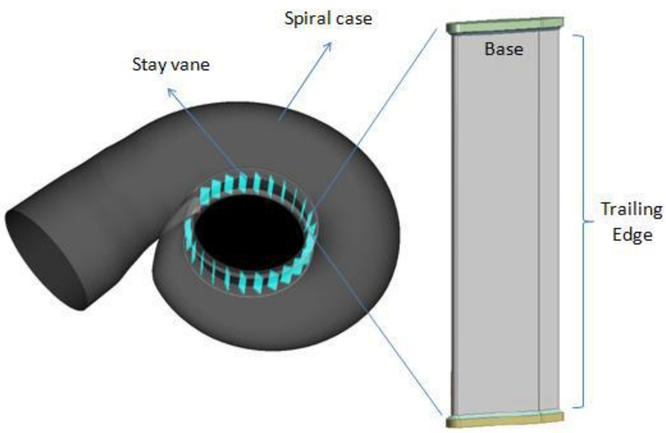

Figure 1. Spiral case and the set of stay vanes. Venturatto, *et. al* (2013)

The main objective of this work is to develop a computational methodology to analyze such vibrations without depending excessively on experimental methods. It can lead to even better profile formats because it makes possible to test different geometries using few resources.

With this goal in mind, we have developed a computational method that uses a moving reference frame solidary to the structure and solves the fluid and the structural equations (rigid bodies elastically mounted) in a coupled manner, so it is possible to evaluate the fluid-structure interaction at each time step. Since we have a non-inertial system fixed to the body, we have to modify the Navier-Stokes and the boundary conditions (see section 2.2). Figure 2 below shows how the variables are related to each other.

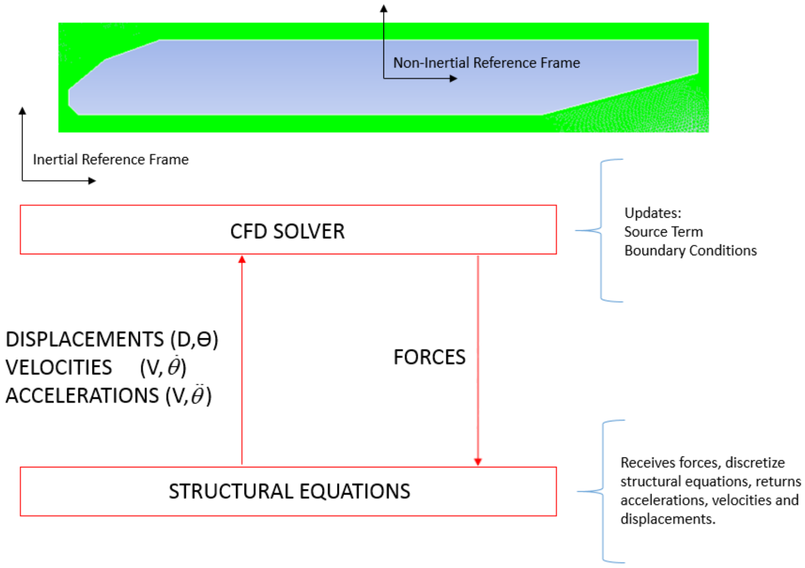

Figure 2. Relationship between flow and structure variables

2. THEORETICAL FORMULATION

The objective of this section is to present some of the concepts employed throughout this paper. The items explore topics related to CFD, such as: finite volume method (section 2.1) and solver corrections for simulations with body motion (section 2.2). Also, we present the forces applied by the flow on the structure due to fluid-structure interaction (section 2.3) and the integration of structural equation (section2.4).

2.1 Finite Volume Method

Once the governing equations are defined, the next step to solve these equations numerically is to discretize them in a certain domain. That is, transform the differential equations in a set of algebraic equations. Each equation expresses the conservation of a transported property in some points of a numerical grid. If the problem is transient, time is discretized as well. The method employed by the solver in this work is called finite volume method. In such method, the governing equations in the conservative form, Eq.(2.1), are integrated over a control volume (CV).

$$\frac{\partial(\rho\phi)}{\partial t}+\nabla.(\rho\phi\vec{v})=\nabla.(\Gamma\nabla\phi)+S_\phi \tag{2.1}$$

where: ϕ is the transported property, Γ is the diffusivity coefficient, $\nabla\equiv\vec{i}\frac{\partial}{\partial x}+\vec{j}\frac{\partial}{\partial y}+\vec{k}\frac{\partial}{\partial z}$ is the gradient operator; $\vec{v}$ is the velocity vector, ρ is the density, S_ϕ is the source term. Applying the Gauss divergence theorem to the convective and diffusive terms of Eq.(2.1), we obtain:

$$\frac{\partial}{\partial t}\left(\int_{CV}\rho\phi dV\right)+\int_A \rho\phi\vec{v}.d\vec{A}=\int_A \Gamma_\phi\nabla\phi.d\vec{A}+\int_{CV}S_\phi dV \tag{2.2}$$

In which integrals over the CV were turned into a flux over the volume faces. Equation (2.2) applied to all cell in a domain lead to the set of algebraic equation below:

$$\frac{\partial(\rho\phi)}{\partial t}V+\sum_f^{Nfaces}(\rho_f\vec{v}_f\phi_f).\vec{A}_f=\sum_f^{Nfaces}\Gamma_\phi(\nabla\phi)_f.\vec{A}_f+S_\phi V \tag{2.3}$$

where: Nfaces: Number of cell faces, ϕ_f value of ϕ convected through face f, $\rho_f \vec{v}_f . \vec{A}_f$ mass flux at face f, $\vec{A}_f$ area vector $(\nabla\phi)_f$ is the ϕ gradient at face f, V cell volume.

Specific information about spatial discretization, gradients and derivatives evaluation, temporal discretization, pressure-velocity coupling and so on can be found on Fluent 15,0 user's Guide (2014).

2.2 Solver correction for simulations with body motion

A broadly employed method in simulations where there is a structure vibrating due the interaction with a flow around it is named ALE (Arbitrary Lagrangian–Eulerian), where the mesh is deformed at each time step. This procedure has a relatively high computational cost and it is more difficult to converge. In situations where the time of simulations is important, for instance a CFD analysis as a part of an optimization process, one should search for methods that demand less time to produce results. One of such methods consists in define a non-inertial reference frame solidary to the body and correct the CFD solver due to this change. In this work, we have a body mounted in an elastic base and a flow exercising forces around it. With a C++ code (the UDF mentioned in section 1), we can solve the structural equations and pass the information obtained from the body motion (displacements, velocity and acceleration) to the solver in order to correct the Navier-Stokes equations (a momentum source term) and the boundary conditions. The way to do that is showed below.

2.2.1 Momentum source term

According to Li, Sherwin and Bearman (2002), the Navier–Stokes correction for a system with a moving reference is given by the Eq.(2.4) , considering a system free to oscillate in both x and y direction and also rotate of an angle theta. See Figure 3. As the momentum equation is divided by ρ, the momentum becomes acceleration.

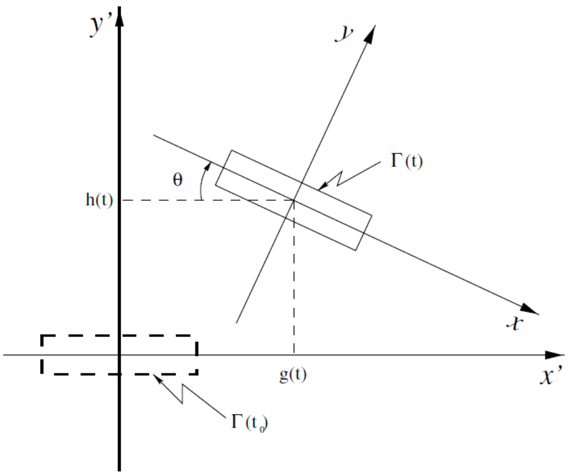

Figure 3. Moving reference frame solidary to a body. Li, Sherwin and Bearman (2002)

$$\frac{\partial \vec{v}}{\partial t} + (\vec{v}.\nabla)\vec{v} = -\nabla p + \nu\nabla^2\vec{v} + [G(\vec{v},t)] \tag{2.4}$$

Where: $[G(\vec{v},t)] = 2\dot{\theta}[I_0]\vec{v} + (\dot{\theta})^2\vec{x} + \ddot{\theta}[I_0]\vec{x} - [A^T][\ddot{d}]$

With: $[I_0] = \begin{pmatrix} 0 & -1 \\ 1 & 0 \end{pmatrix}, [\mathrm{A}^T] = \begin{pmatrix} \cos\theta & -\sin\theta \\ \sin\theta & \cos\theta \end{pmatrix}, [\ddot{\mathrm{d}}] = (\ddot{\mathrm{g}}(\mathrm{t}), \ddot{\mathrm{h}}(\mathrm{t}))^T, t = time, \vec{x} = displacement$

The dot over the variables represents a time derivative, x'y' the fixed reference frame and xy the moving reference frame.

2.2.2 Boundary conditions correction

Two types of boundary conditions may change with the motion of the body. Inlet (Dirichlet) and Outlet (Neuman). We present below the relationship between these conditions in systems xy e x'y'.

2.2.2.1 Dirichlet

Differentiating the following relation $\vec{x}\,' = \vec{d} + [A]\vec{x}; \vec{x} = [A^T](\vec{x}\,' - \vec{d})$, we obtain:

$$\vec{v} = \dot{\theta}[I_0]\vec{x} + [A^T](\vec{v}\,' - \vec{d}) \tag{2.5}$$

Where $\vec{v}\,'$ is the velocity in the far-field measured in the fixed system.

2.2.2.2 Neumann

One can prove that for the outlet, where the Neumann condition is applied, the velocity gradient normal to boundary is given by:

$$\nabla \mathrm{u}.\vec{n} = g_N^{u'} - \dot{\theta}n_y; \nabla \mathrm{v}.\vec{n} = g_N^{v'} - \dot{\theta}n_x \tag{2.6}$$

Where $g_N^{u'}$ and $g_N^{v'}$ are known function. If there is no rotation of the body or it is too small, the Neumann condition does not change even though the body is moving. This is the case presented in the results, on section 4.

2.3 Forces in Fluid Structure Interaction

The forces applied on the body by the fluid are due to pressure and viscous stresses, and are given by Eq (2.7). Since the only degree of freedom employed is y, we present only the force in the normal direction to flow.

$$F_y = F_{py} + F_{vy} = p\delta A_y + \mu\left(2\frac{\partial v}{\partial y}\delta A_y + \left(\frac{\partial u}{\partial y} + \frac{\partial v}{\partial x}\right)\delta A_x + \left(\frac{\partial w}{\partial y} + \frac{\partial v}{\partial z}\right)\delta A_z\right) \tag{2.7}$$

2.4 Dimensionless structure equation and time discretization

The dimensionless form of the mass-spring-damper equation for the structure is given as follows:

$$M^*\ddot{y}^* + C^*\dot{y}^* + K^*y^* = F_y^* \tag{2.8}$$

Where M* is the dimensionless mass of the system, C* is the dimensionless damping of the system and K* is the dimensionless stiffness. Fy* is the force in the transversal direction.

These variables are related to the dimension variables according the relationships below. U_∞ is the velocity at the bulk flow, D is the stay vane chord, L is the depth, ρ is the water specific mass, M is the structure mass and t, time. C_L is the lifting coefficient.

$$M^* = \frac{M}{\rho D^2 L}, C^* = \frac{C}{\rho U_\infty DL}, K^* = \frac{K}{\rho U_\infty{}^2 L}, F_y{}^* = \frac{C_L}{2} = \frac{F_y}{\rho U_\infty{}^2 DL} \tag{2.9}$$

The variables $\ddot{y}^*$, $\dot{y}^*$ and y^* are the displacements, velocities and accelerations and are related to the dimension variables as follows:

$$\ddot{y}^* = \frac{\ddot{y}D}{U_\infty{}^2}, \dot{y}^* = \frac{\dot{y}}{U_\infty}, y^* = \frac{y}{D} \tag{2.10}$$

A different approach to define M*, C* and K* is to relate these variables with m*(mass ratio), ζ (damping ratio) and V_r (reduced velocity). These dimensionless terms are very common in literature when it comes to experiments/ simulations with the cylinder:

$$m^* = \frac{4M}{\rho\pi D^2 L}, \zeta = \frac{C}{2\sqrt{KM}}, V_r = \frac{U_\infty}{f_n D} = \frac{2\pi U_\infty}{\sqrt{\frac{K}{M}} D}, M^* = \frac{\pi m^*}{4}, C^* = \frac{\pi^2 m^* \zeta}{V_r}, K^* = \frac{\pi^3 m^*}{V_r^2} \tag{2.11}$$

Finally, a time discretization of the Eq. (2.8) must be obtained in order to get the structural variables at each time step of the solution. The method employed was also adopted by Neto (2007). The degree of freedom employed in this case is y, since both the vibration in the streamwise direction and the rotation are negligible.

$$\dot{y}^*(t^* + \Delta t^*)\left(\frac{M^*}{\Delta t^*} + \frac{C^*}{2} + \frac{K^*\Delta t^*}{4}\right) = \dot{y}^*(t^*)\left(\frac{M^*}{\Delta t^*} - \frac{C^*}{2} - \frac{K^*\Delta t^*}{4}\right) - K^* y^*(t^*) + \frac{F_y^*(t^* + \Delta t^*) + F_y^*(t^*)}{2} \tag{2.12}$$

3. COMPUTATIONAL MODELING

The CFD code used to perform flow calculations was ANSYS Fluent, and a C++ code, called UDF (Used Defined Function) was written in order to correct some aspects of the solver and solve the structural equations, as mentioned before. All cases were set for a transient, two-dimensional simulation.

Firstly, a fixed body simulation was carried out in order to correctly evaluate the parameters of the simulation per se (mesh, time step, turbulence model, P-V coupling, etc.). Afterwards, the moving stay vane was simulated for Re = 8× 10^6, same value adopted for the fixed case. All cases were simulated with U_∞=1 and D=1 (stay vane chord). The density was $\rho = 1$. Therefore, the dynamic viscosity was defined by $\mathrm{Re} = \mu^{-1}$. The stay vane computational model is showed below, in

Figure **4**. This stay vane is from CESP's Ilha Solteira Power Plant and it is the base for this work.

Figure 4. Stay vane computational model. Source: CESP.

The turbulence model employed was k-ω SST and the cell fluxes calculated by a second order upwind scheme.

4. RESULTS

4.1 Fixed stay vane – Re=8x10^6.

The results bin this section come from a mesh with 174906 faces, 68474 nodes e 106462 cells. The dimensions are: Xmin=-2.5, Xmax=5.5, Ymin=-1.1 e Ymax=1.2, consistent with the space that 1 out of 24 stay vanes occupies around the stay ring. The time step is 5 x 10^{-3} s, the inlet is a velocity-inlet type (velocity prescribed, pressure free) and outlet an outflow type (velocity gradient normal to boundary equal zero, pressure equal zero). Two periodic conditions were defined in the parallel direction to the stay vane chord. They simulate the influence of the other neighbor vanes. The first element height in the boundary layer was defined so y+=1 for this element. An attack angle of 58º is defined on the inlet, according to the angle the flow comes from the spiral case.

The vorticity contours (Figure 5) and the Strouhal number (Figure 6) are presented below. Strouhal number gives an idea of the vortex shedding frequency and, therefore, weather the vortex can cause or not resonance in the structure. We can notice that not a single dominant frequency is present and the higher frequency (downstream the trailing edge) with St=0.17.

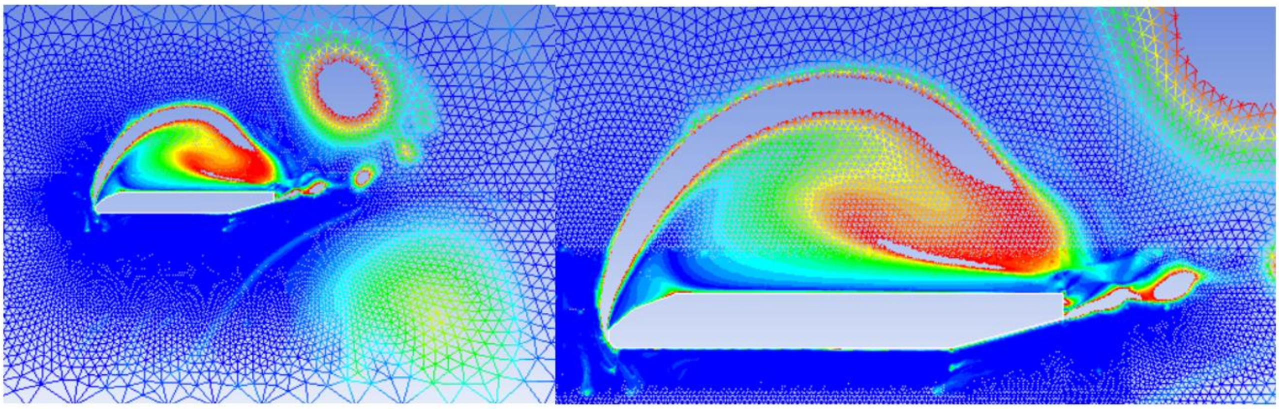

Figure 5. Vorticity contours for the fixed stay vane simulation Re=8x10^6

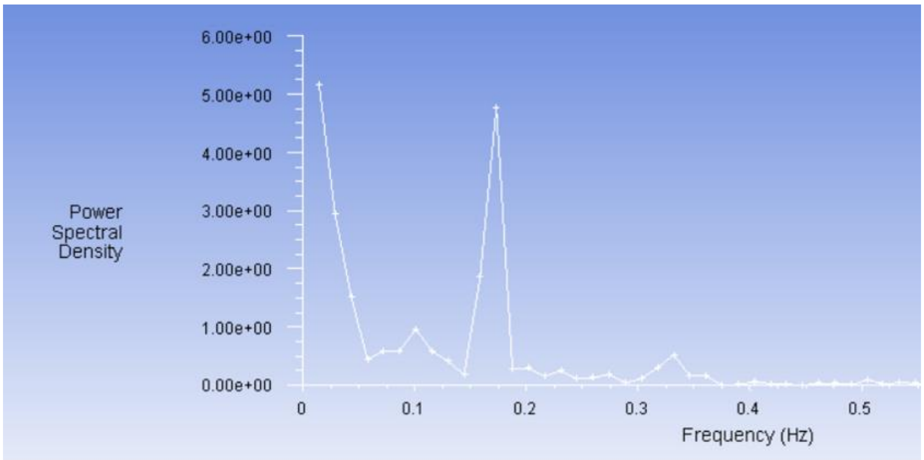

Figure 6. Strouhal number for fixed stay vane. The higher frequency (downstream the trailing edge) has St=0.17

4.2 Moving stay vane – Re=8x10^6.

Following the same characteristics of the fixed case above (size of domain, mesh, boundary condition, etc), we present below in Figure 7 the results for the displacements in the normal direction related to flow, y, that is used to evaluate the effects of resonance in the vanes. The value of V_r ,defined in section 2.4, was assumed to be 5. In Figure 8 we can see the Strouhal number for the moving case, which is similar to the previous fixed case (St=0.16). Therefore, this is the region of frequencies to pay attention in case of resonance problems.

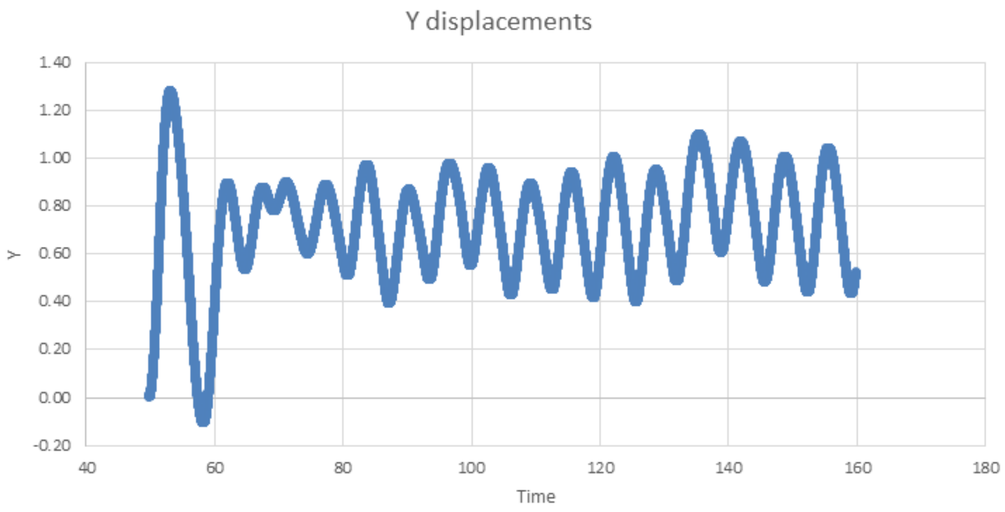

Figure 7: Displacements in y

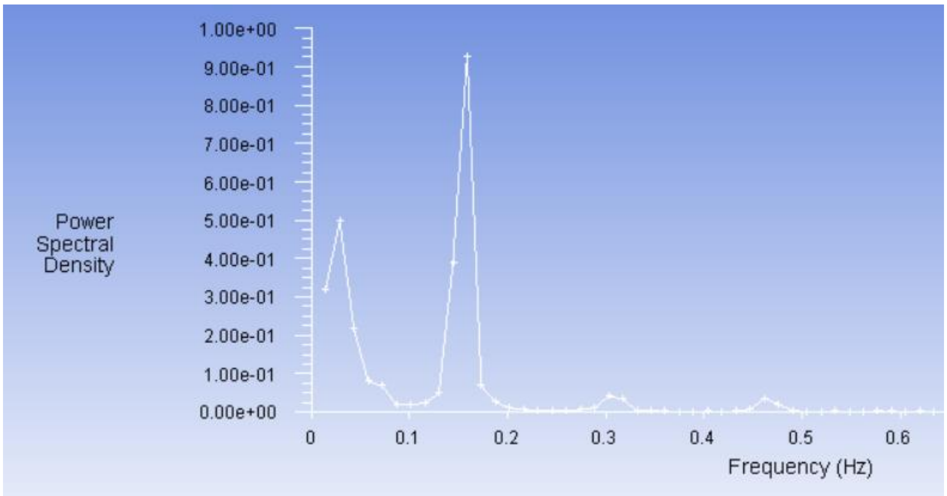

Figure 8. Strouhal number for moving stay vane. The higher frequency (downstream the trailing edge) has St=0.16.

5. CONCLUSIONS

We have presented in this article a methodology to analyze the vortex induced vibrations in a given structure mounted over an elastic base, using a commercial CFD code (Fluent) associated to a C++ code, used to correct some aspects in the solver and to solve the structural equation numerically, at each time step. The methodology for the flow around the stay vane was successfully already applied. A future work could try to combine this CFD analyses with an optimization process so it is possible to reach a satisfactory design automatically.

6. REFERENCES

ANSYS. “Fluent User’s Guide”. Release 15.0. [S.l.]: Ansys Inc., 2014.

BEARMAN, P.W. “Vortex Shedding From Oscillating Bluff Bodies.” *Anual Review Fliud Mechanics*, 1984: 195-222.

CARMO, B.S. *On Wake Interference in the Flow around Two Circular Cylinders:Direct Stability Analysis and Flow Induced Vibrations.* London: Doctor Degree, Imperial College London, Department of Aeronautics, 2009.

GISSONI, H.C. *“Análise mecânica de vibrações em travessas do pré-distribuidor de turbinas hidráulicas”, Dissertação (Mestrado).* São Paulo: EPUSP, 2005.

KURIHARA, F., H. POLL, D. DIAS, e H. GISSONI. “Diagnóstico de Máquinas para a eliminação da origem de trincas em pré-distribuidores:a otimização da UHE Capivara.” *XIX SNPTEE.* Rio de Janeiro, 2007.

LI, L.,SHERWIN, S.J.,BEARMAN,P.W. “A moving frame of reference algorithm for fuid/structure interaction of rotating and translating bodies.” *International Journal for Numerical Methods In Fluids*, 2002: 187-206.

NETO, A. D'A.GOSTINI. *"Estudo de Vibrações induzidas por escoamento em pré-distribuidores de turbinas hidráulicas utilizando CFD".* São Paulo: Trabalho de Formatura - Escola Poltécnica da Universidade de São Paulo - Departamento de Engenahria Mecânica, 2007.

ROSHKO, A. "Experiments on the flow past a circular cylinder at very high Reynolds number." *Journal Fluid Mechanics,* 1961: 10:345-356.

SARPKAYA, T. "A critical review of the intrinsic nature of vortex-induced." *Journal of Fluids and Structures*, 26 de January de 2004: 389-447.

SCHEWE, G. "On the force fluctuations acting on a circular cylinder in cross-flow subcritical up to transcritical Reynolds Numbers." *Journal Fluid Mechanics*, 1983: 133:265-285.

VENTURATTO, R.J. *Otimização paramétrica considerando interação fluido-estrutura de um pré-distribuidor de turbina hidráulica.* São Paulo: Trabalho de Formatura,Departamento de Engenharia Mecatrônica e Sistemas Mecânicos., 2012.

WILLIAMSON, C.H.K.,Govardhan R. "Vortex Induced Vibrations." *Annual Review Fluid Mechanics*, 2004: 413-455.

ZOBEIRI, A.,AUSONI,P.AVELLAN,F.,FARHAT,M. "Vortex Shedding From Blunt And Oblique Trailing Edge Hydrofoils." *3rd IAHR International Meeting of the Workgroup on Cavitation and Dynamic Problems in Hydraulic Machinery and Systems.* Brno, 2009.

7. RESPONSIBILITY NOTICE

The authors are the only responsible for the printed material included in this paper.